

1 **Calvin cycle mutants of photoheterotrophic purple non-sulfur bacteria fail to grow**
2 **due to an electron imbalance rather than toxic metabolite accumulation**

3

4

5 Running title: Calvin cycle roles during photoheterotrophic growth

6

7 Gina C. Gordon^{1*} and James B. McKinlay^{2#}

8 ¹Biotechnology Undergraduate Program, Indiana University, Bloomington, Indiana, USA

9 ²Department of Biology, Indiana University, Bloomington, Indiana, USA

10 *current address: Microbiology Doctoral Training Program, University of Wisconsin,

11 Madison, Wisconsin, USA

12 # Corresponding author: jmckinla@indiana.edu

13 **ABSTRACT**

14 Purple nonsulfur bacteria grow photoheterotrophically by using light for energy and
15 organic compounds for carbon and electrons. Disrupting the activity of the CO₂-fixing
16 Calvin cycle enzyme, ribulose-1,5-bisphosphate carboxylase (Rubisco), prevents
17 photoheterotrophic growth unless an electron acceptor is provided or if cells can dispose
18 of electrons as H₂. Such observations led to the long-standing model wherein the Calvin
19 cycle is necessary during photoheterotrophic growth to maintain a pool of oxidized
20 electron carriers. This model was recently challenged with an alternative model wherein
21 disrupting Rubisco activity prevents photoheterotrophic growth due to the accumulation
22 of toxic ribulose-1,5-bisphosphate (RuBP) (Wang, D., Y. Zhang, E. L. Pohlmann, J. Li,
23 and G. P. Roberts. 2011. J. Bacteriol. **193**:3293-3303). Here we confirm that RuBP
24 accumulation can impede the growth of *Rhodospirillum rubrum* and *Rhodopseudomonas*
25 *palustris* Δ Rubisco mutants under conditions where electron carrier oxidation is coupled
26 to H₂ production. However, we also demonstrate that *Rs. rubrum* and *Rp. palustris* Calvin
27 cycle phosphoribulokinase mutants that cannot produce RuBP cannot grow
28 photoheterotrophically on succinate unless an electron acceptor is provided or H₂
29 production is permitted. Thus, the Calvin cycle is still needed to oxidize electron carriers
30 even in the absence of toxic RuBP. Surprisingly, Calvin cycle mutants of *Rs. rubrum*, but
31 not of *Rp. palustris*, grew photoheterotrophically on malate without provided electron
32 acceptors or H₂ production. The mechanism by which *Rs. rubrum* grows under these
33 conditions remains to be elucidated.

34 INTRODUCTION

35 Purple non-sulfur bacteria (PNSB) are renowned for their ability to employ versatile
36 metabolic modules to thrive under different growth conditions. PNSB can grow
37 photoautotrophically using light for energy, inorganic compounds other than water (e.g.,
38 thiosulfate, Fe^{2+}) for electrons, and CO_2 for carbon. The Calvin cycle is well-known for
39 permitting autotrophic growth by converting CO_2 into organic precursors for biosynthesis
40 (Fig 1). In this pathway phosphoribulokinase (PRK) expends ATP to generate ribulose
41 1,5-bisphosphate (RuBP). RuBP is then combined with CO_2 via ribulose 1,5-
42 bisphosphate carboxylase (Rubisco) resulting in two 3-phosphoglycerate. CO_2 fixation
43 generates relatively oxidized metabolites that accept electrons from NAD(P)H via
44 glyceraldehyde-3-phosphate dehydrogenase.

45

46 PNSB can also grow photoheterotrophically using light for energy and organic
47 compounds for carbon and electrons. Unlike in a respiring heterotroph, reducing power
48 from oxidative pathways (e.g., NAD(P)H) is not used to reduce a terminal electron
49 acceptor and generate ATP by oxidative phosphorylation. Rather, ATP generation is
50 largely decoupled from the oxidative pathways of central metabolism as
51 photoheterotrophs repeatedly energize electrons and shuttle them through a H^+ -pumping
52 electron transfer chain to generate ATP by cyclic photophosphorylation (Fig. 1).
53 Nevertheless, the photoheterotrophs generate ample reducing power that must be
54 oxidized to replenish pools of oxidized electron carriers (e.g., NAD(P)^+) and maintain
55 metabolic flow. CO_2 fixation was first hypothesized to fulfill this essential role of
56 maintaining oxidized electron carriers during photoheterotrophic growth in 1933 by

57 Muller (1), prior to the elucidation of the Calvin cycle itself (2) (Fig. 1, Model 1). Muller
58 devised this hypothesis to explain why there was net CO₂ fixation when PNSB grew
59 photoheterotrophically on compounds like butyrate, that are more electron rich than the
60 average carbon in biomass (1). Supporting this hypothesis, it was later shown that PNSB
61 could be grown photoheterotrophically on butyrate without added CO₂ if an electron
62 acceptor like dimethylsulfoxide (DMSO) was provided (3) or if PNSB were allowed to
63 dispose of electrons as H₂ (4). More compelling, deleting genes encoding Rubisco (i.e.,
64 *cbbM* and in some cases *cbbLS*) in model PNSB, including *Rhodobacter sphaeroides*,
65 *Rhodobacter capsulatus* and *Rhodospseudomonas palustris*, prevented photoheterotrophic
66 growth, even with relatively oxidized substrates, unless an alternative electron acceptor
67 was provided (5–7), if electrons were disposed of as H₂ (8), or if an alternative reductive
68 CO₂-fixing pathway was available (9). ¹³C-Labeling experiments with *Rp. palustris* have
69 since shown that the Calvin cycle is one of the most active pathways during
70 photoheterotrophic growth, and it oxidizes 40-60% of the reducing power even during
71 growth with relatively oxidized substrates (8, 10). Thus, there is a long history of
72 evidence to support a model wherein the Calvin cycle plays an essential role in oxidizing
73 excess reducing power generated during photoheterotrophic growth (Fig. 1, Model 1).

74

75 This electron-balancing role of the Calvin cycle was recently called into question. Wang
76 et al showed that the deletion of the Rubisco gene, *cbbM*, in *Rhodospirillum rubrum*,
77 resulted in poor photoheterotrophic growth on malate but oddly did not prevent growth
78 (11). Disrupting Rubisco activity resulted in the accumulation of RuBP, the product of
79 the preceding Calvin cycle enzyme, PRK (Fig. 1). A strong inverse correlation between

80 RuBP levels and growth rate suggested that RuBP was toxic (11). When the gene
81 encoding PRK, *cbbP*, was deleted in a Δ Rubisco mutant to prevent RuBP production, a
82 wild-type growth rate was restored (11). Wang et al proposed that the previously
83 observed inability of various PNSB Δ Rubisco mutants to grow photoheterotrophically
84 was due to the accumulation of toxic RuBP rather than an electron imbalance (Fig. 1,
85 Model 2). In advocacy of this alternative hypothesis, we note that the addition of
86 alternative electron acceptors or permitting the disposal of electrons as H₂ has been
87 shown to result in lower Calvin cycle transcript levels in multiple PNSB (5, 8, 10, 12).
88 Thus, simply providing electron acceptors and permitting H₂ production could repress
89 Calvin cycle activity and prevent toxic RuBP accumulation.

90
91 Even so, we were skeptical of this alternative model for several reasons. First, ¹³C-
92 metabolic flux and flux balance analyses agree that disrupting Calvin cycle activity
93 should lead to a lethal depletion of oxidized electron carriers, or in other terms, a lethal
94 excess of reducing power (8, 10, 13, 14). Electron balance must be maintained to support
95 metabolic flow and cell viability. Second, deleting the gene encoding the RuBP-
96 producing PRK enzyme, *cbbP*, was previously shown to prevent photoheterotrophic
97 growth in *Rb. sphaeroides* (12) and *Rb. capsulatus* (15). Adding the electron acceptor,
98 DMSO, or allowing the cells to produce H₂ restored growth, supporting the original
99 model since these Δ PRK Calvin cycle mutants cannot produce RuBP (12, 15). Third, the
100 experiments by Wang et al were performed in a medium that contained glutamate as the
101 sole nitrogen source (11), which is known to induce H₂ production via the enzyme,
102 nitrogenase (16). When H₂ production was repressed by using NH₄⁺ as the nitrogen

103 source, the same *Rs. rubrum* Δ Rubisco mutant displayed questionable photoheterotrophic
104 growth (achieved 10% of the wild-type final OD) (17). Furthermore, another *Rs. rubrum*
105 Δ Rubisco mutant previously shown to grow photoheterotrophically with NH_4^+ (18) was
106 later shown to produce H_2 due to the acquisition of a *nifA** mutation that bypassed the
107 repression of nitrogenase by NH_4^+ , resulting in H_2 production (17). We suspected that
108 photoheterotrophic growth of *Rs. rubrum* observed by Wang et al (11) was only possible
109 due to the disposal of electrons as H_2 .

110

111 The purpose of this study was to reexamine the impact of electron imbalance versus
112 RuBP accumulation on PNSB photoheterotrophic growth. To distinguish between
113 phenotypes that might be unique to *Rs. rubrum* versus those that might be more broadly
114 applicable to PNSB we performed experiments on Δ PRK and Δ Rubisco mutants of *Rs.*
115 *rubrum* and *Rp. palustris*. Furthermore, we employed two different carbon sources that
116 have different numbers of available electrons, malate ($12 e^-$) and succinate ($14 e^-$), but are
117 both expected to enter metabolism and be processed by the TCA cycle (10). We
118 confirmed the observations of Wang et al (11) that Δ Rubisco mutations can impede
119 growth rates, likely through the accumulation of toxic RuBP. However, we also
120 confirmed the original model wherein an alternative means of electron disposal is
121 required for photoheterotrophic growth in the absence of the Calvin cycle. Surprisingly,
122 *Rs. rubrum* appears to have an alternative mechanism than H_2 production that permits
123 photoheterotrophic growth of Calvin cycle mutants with malate but not with succinate.

124

125 **MATERIALS AND METHODS**

126 **Strains and Growth Conditions.** All strains are summarized in Table 1. *Rs. rubrum*
127 strains were derived from strain UR2 (19) and were provided by Gary Roberts,
128 University of Wisconsin, Madison. *Rs. rubrum* genotypes were verified by PCR using
129 primers that were either flanking or internal to the mutated region. *Rs. rubrum* strains
130 were streaked to supplemented malate-ammonium (SMN) (19) agar plates from 10%
131 DMSO frozen stocks and grown aerobically in darkness at 30°C. 5-mL aerobic SMN
132 cultures were inoculated from single colonies and incubated at 30°C with shaking.
133 Aerobic starter cultures were used to inoculate 10 mL of anaerobic defined medium in
134 28-ml anaerobic test tubes. The defined medium was based on a previously described
135 recipe (20) and contained (per liter) 0.9 g K₂HPO₄, 0.6 g KH₂PO₄, 0.1 g MgSO₄, 0.075 g
136 CaCl₂*2H₂O, 0.012 g FeSO₄*7H₂O, 0.02 g EDTA, 0.015 g biotin, 1ml of trace elements
137 (20), and either 5.9 mM of sodium glutamate to permit H₂ production or 7.5 mM of
138 (NH₄)₂SO₄ to prevent H₂ production. DMSO was added to a final concentration of 60
139 mM where indicated. Culture medium was made anaerobic by bubbling media with Ar
140 gas and then sealing tubes with rubber stoppers (Geo-Microbial Technologies, Ochelata,
141 OK) and aluminum crimps. Cultures were incubated at 30°C in front of a 60W light bulb.
142 *Rp. palustris* strains were derived from the type strain CGA009 (21), which is defective
143 for uptake hydrogenase activity (22). *Rp. palustris* was grown in a similar manner to *Rs.*
144 *rubrum* except in a defined photosynthetic medium which always contained (NH₄)₂SO₄ as
145 the nitrogen source (23). H₂ production was accomplished for *Rp. palustris* using a *nifA**
146 background (Table 1) that allows for H₂ production in the presence of NH₄⁺ (8).
147 Disodium salts of fumarate, malate or succinate were used as carbon sources for all
148 defined media at a final concentration of 10 mM. *R. rubrum* growth experiments in media

149 with succinate and NH_4^+ were inoculated from starter cultures that were grown
150 photoheterotrophically with malate and NH_4^+ . *Escherichia coli* was grown on LB agar or
151 in LB broth. Gentamycin and kanamycin were used at 100 $\mu\text{g}/\text{ml}$ each for *Rp. palustris*,
152 at 10 $\mu\text{g}/\text{ml}$ each for *Rs. rubrum*, and at 10 $\mu\text{g}/\text{ml}$ and 30 $\mu\text{g}/\text{ml}$, respectively, for *E. coli*.
153 Antibiotics were used on plates and in starter cultures but were omitted during
154 experiments in which growth rates were compared (including for strains carrying
155 plasmids).

156

157 ***Rp. palustris* strain construction.** In-frame deletions of *cbbLS*, encoding type I Rubisco,
158 and *cbbP*, encoding PRK, were constructed using primers and plasmids listed in Table 2
159 as described (22). Briefly, regions ~1kb upstream and downstream of the gene to be
160 deleted were amplified by PCR. The two PCR products were combined in-frame by
161 overlap extension PCR (24) and cloned into either pGEM (Promega, Madison, WI) or
162 pUC19 (25) using the indicated restriction sites (Table 2) and maintained in *E. coli*
163 NEB10 β (New England Biolabs, Ipswich, MA). Constructs were confirmed by
164 sequencing to ensure that no point mutations were introduced. The Km^{R} cassette from
165 pPS858_Km2 was amplified and inserted at a KpnI site within the ΔcbbP construct.
166 Deletion constructs were then subcloned into the *Rp. palustris* suicide vector pJQ200SK
167 (26), maintained in *E. coli* S17 (27), and transferred to *Rp. palustris* by conjugation.
168 Counterselection on agar plates supplemented with 10% sucrose and screening for
169 sensitivity to gentamycin were used to obtain recombinant *Rp. palustris* strains.
170 Genotypes were confirmed by PCR. To complement the $\Delta\text{cbbP}::\text{Km}^{\text{R}}$ mutation in the *Rp.*
171 *palustris* ΔPRK strain, CGA4007, the *cbbP* gene and the native ribosomal binding site

172 were amplified using primers listed in Table 2, cloned into pGEM, sequenced, and then
173 subcloned into the *Rp. palustris* constitutive expression vector, pBBPgdh (8) in *E. coli*
174 NEB10 β . The vector was then moved into *E. coli* S17 and transferred into CGA4007 by
175 conjugation.

176

177 **Analytical techniques.** Cell density was assayed by optical density at 660 nm (OD₆₆₀)
178 using a Genesys 20 visible spectrophotometer (Thermo-Fisher, Pittsburgh, PA). Specific
179 growth rates were determined using measurements with values that were < 0.8 OD₆₆₀
180 where a linear relationship between cell density and OD₆₆₀ was maintained. H₂ was
181 sampled from culture headspace using a gas-tight syringe and analyzed using a Shimadzu
182 GC-2014 gas chromatograph as described (28). Polyhydroxybutyrate was hydrolyzed
183 from dry cells and extracted as crotonic acid by boiling cells in 1 ml of pure sulfuric acid
184 in screw-cap glass test tubes. Extracts were diluted with 4 ml water, centrifuged, filtered,
185 diluted 10-fold with water, and then crotonic acid was quantified by HPLC (Shimadzu) as
186 described (29). Culture supernatants were analyzed for formate using the same HPLC
187 parameters.

188

189 **RESULTS AND DISCUSSION**

190 **Preventing RuBP accumulation in Δ Rubisco mutants improves growth rates under**
191 **conditions permitting H₂-production.** Previously, Wang et al proposed that PNSB
192 Rubisco mutants fail to grow due to the toxic accumulation of RuBP (11). This served as
193 an alternative hypothesis to the long-standing model that disrupting the Calvin cycle
194 prevents photoheterotrophic growth by preventing the oxidation of reduced electron

195 carriers (Fig. 1). We were concerned that the growth conditions used by Wang et al (11)
196 permitted the disposal of excess electrons as H₂, and therefore were unsuitable to rule out
197 the original model. To confirm that H₂ was produced and to verify the growth trends
198 observed by Wang et al (11) we grew the same *Rs. rubrum* strains from the Wang et al
199 study (UR2, UR2565, UR5251, and UR2557; Table 1) with malate and glutamate, the
200 latter being a nitrogen source that permits H₂ production via nitrogenase. We observed
201 over a mmole of H₂ production from all strains during the growth phase (Fig. 2A). As
202 was observed previously, the *Rs. rubrum* Δ Rubisco mutant, UR5251, grew more slowly
203 than the wild-type strain (UR2), at 45% of the wild-type growth rate (Fig. 2B). The
204 Δ PRK mutant grew at the same rate as the wild-type strain (Fig. 2B). Deleting the gene
205 encoding PRK, *cbbP*, in a Δ Rubisco background restored the growth rate to a wild-type
206 level (Fig. 2B). Interestingly, the Δ Rubisco mutant growth rate was more variable than
207 for other strains (Fig. 2B), perhaps due to selective pressure for variants that produce less
208 RuBP.

209

210 We also performed the same experiment with *Rp. palustris* using a *nifA** genetic
211 background, succinate as the carbon source, and with NH₄⁺ as the nitrogen source. *NifA**
212 strains produce H₂ in the presence of NH₄⁺ (8). Similar to what was observed for *Rs.*
213 *rubrum*, the *Rp. palustris* *NifA** Δ Rubisco strain exhibited a severely impaired growth
214 rate (56% that of the *NifA** parent) whereas the *NifA** Δ PRK strain had a growth rate
215 that was 83% that of the parent (Fig. 3). Deleting the gene encoding PRK, *cbbP*, in the
216 *NifA** Δ Rubisco mutant improved the growth rate of the Δ Rubisco mutant to a similar
217 level observed in the *NifA** Δ PRK strain (91% that of the *NifA** parent; Fig. 3). Thus,

218 our results support the notion that RuBP accumulation can negatively impact
219 photoheterotrophic growth rates in other PNSB. However, since these experiments
220 permitted the disposal of excess electrons as H₂, they did not rule out the original model
221 wherein electron imbalance prevents photoheterotrophic growth of Calvin cycle mutants.

222

223 ***Rs. rubrum* Calvin cycle mutants are capable of photoheterotrophic growth with**
224 **malate or fumarate but not with succinate.** Several studies have demonstrated that
225 PNSB Calvin cycle mutants, including Δ PRK mutants of *Rb. sphaeroides* and *Rb.*
226 *capsulatus*, cannot grow photoheterotrophically with compounds such as malate,
227 succinate, and acetate, unless electron acceptors were added or H₂ production was
228 permitted (6–8, 12, 15). To verify that Calvin cycle PRK activity is essential for
229 photoheterotrophic growth we made a *Rp. palustris* Δ PRK mutant and tested for growth
230 under conditions that repress H₂ production via nitrogenase. This *Rp. palustris* Δ PRK
231 mutant was incapable of photoheterotrophic growth with malate and NH₄⁺ unless *cbbP*,
232 the gene encoding PRK, was expressed in trans (Fig. 4, Δ PRK pBBP*cbbP*) or if H₂
233 production was permitted (Fig. 4, NifA* Δ PRK). The same trends were observed when
234 succinate was used in place of malate (data not shown).

235

236 Based on observations that PRK is critical for photoheterotrophic growth with NH₄⁺ in *R.*
237 *palustris* (Fig. 4), *Rb. sphaeroides* (12), and *Rb. capsulatus* (15) we expected that *Rs.*
238 *rubrum* Calvin cycle mutants would also not grow with NH₄⁺. However, we observed
239 growth of the *Rs. rubrum* Calvin cycle mutants to approximately the same final OD as the
240 wild-type strain under phototrophic conditions with malate and NH₄⁺ (Fig. 5). We

241 confirmed that growth was not due to contaminating bacteria through PCR amplification
242 of genes encoding Rubisco and PRK both before and after growth experiments. The
243 Δ Rubisco mutant, UR5251, showed an initial lag phase under phototrophic conditions
244 with malate and NH_4^+ (Fig. 5). However, this lag phase was not the result of an
245 adaptation to anaerobic conditions as it was not observed again after transferring cultures
246 to rich aerobic medium and then back into anaerobic phototrophic conditions with malate
247 and NH_4^+ (Fig 5). The lag phase was also not observed again when the Δ Rubisco mutant
248 was transferred directly from anaerobic phototrophic conditions with malate and NH_4^+ to
249 identical conditions (data not shown). Thus, there may have been selective pressure for
250 suppressor mutations that limit the production of toxic RuBP by the Δ Rubisco mutant.
251 Such a mutation could explain the difference between our observations and those
252 previously where the Δ Rubisco mutant, UR5251, only grew to ~10% of the final OD of
253 the wild-type when supplied with malate and NH_4^+ (17).

254

255 Even though *Rs. rubrum* Calvin cycle mutants unexpectedly grew with malate and NH_4^+
256 they did not grow with succinate and NH_4^+ unless DMSO was provided as an electron
257 acceptor (Fig. 6). For these experiments, medium with succinate and NH_4^+ was
258 inoculated with strains that were previously grown phototrophically with malate and
259 NH_4^+ (Fig. 5). The DMSO requirement for growth with succinate but not with malate
260 suggests that *Rs. rubrum* Calvin cycle mutants have an additional mechanism to maintain
261 electron balance when grown on malate but not on succinate. It is possible that this
262 mechanism cannot oxidize the extra reducing power produced during the metabolism of
263 succinate, since succinate has two more available electrons than malate. In support of this

264 notion, all *Rs. rubrum* Calvin cycle mutants grew phototrophically with fumarate and
265 NH_4^+ (data not shown). Fumarate has the same number of available electrons as malate
266 and is also expected to be processed by the TCA cycle (10).

267

268 Several mechanisms are possible that could allow *Rs. rubrum* Calvin cycle mutants to
269 grow photoheterotrophically with NH_4^+ , some of which we can rule out while others we
270 can only speculate on. Mutations in *nifA* that allow for constitutive H_2 production (17, 30,
271 31) can be ruled out as we did not detect H_2 in any of the *Rs. rubrum* Calvin cycle mutant
272 cultures grown with malate and NH_4^+ . Production of polyhydroxybutyrate storage
273 polymer as an electron sink can also be ruled out as we did not detect any
274 polyhydroxybutyrate in any *Rs. rubrum* strain grown with malate and NH_4^+ . A flux
275 balance model predicted that a *Rs. rubrum* Calvin cycle mutant could grow
276 photoheterotrophically with malate by producing formate but that formate production
277 would not satisfy electron balance nor permit growth with succinate (13). However, we
278 did not detect formate in the supernatants of any *Rs. rubrum* culture.

279

280 A mechanism we can currently only speculate on is the use of an alternative CO_2 -fixing
281 pathway in *Rs. rubrum* that could substitute for the Calvin cycle. In support of such a
282 mechanism, a *Rs. rubrum* $\Delta\text{Rubisco}$ strain was previously reported to grow with CO_2 as
283 the sole carbon source and with thiosulfate as an electron donor, though the CO_2 -fixing
284 pathway responsible was not identified (32). One possibility is the ethylmalonyl-CoA
285 pathway, which permitted phototrophic growth of *Rb. sphaeroides* $\Delta\text{Rubisco}$ mutants
286 with acetate and NH_4^+ (9). However, the ethylmalonyl-CoA pathway is unlikely to permit

287 photoheterotrophic growth of PNSB Calvin cycle mutants with malate since excessive
288 reducing power would be made en route to the start of the pathway (9, 13). Indeed, the
289 *Rb. sphaeroides* Rubisco mutant that grew with acetate and NH_4^+ did not grow with
290 malate and NH_4^+ (9). Another possibility for a CO_2 -fixing pathway is the reverse TCA
291 cycle. A flux balance model predicted that the reverse TCA cycle could substitute for the
292 Calvin cycle in maintaining electron balance in *Rs. rubrum* (13). Consistent with this
293 possibility, fumarate reductase activity was previously detected in *Rs. rubrum* under
294 anaerobic conditions (33). However, it is not clear whether reverse TCA cycle flux could
295 explain growth with malate and fumarate but not with succinate.

296

297 The mechanism that permits *Rs. rubrum* Calvin cycle mutants to grow phototrophically
298 on malate without producing H_2 remains to be elucidated. Even so, the fact that *Rs.*
299 *rubrum* ΔPRK mutants, which cannot produce RuBP, still require an electron acceptor to
300 grow on succinate (Fig. 6), and that similar observations have been made for ΔPRK
301 mutants of *R. palustris* (Fig. 4) and other PNSB (12, 15) with succinate and malate,
302 indicate that RuBP accumulation is not the reason why Calvin cycle mutants fail to grow
303 photoheterotrophically. Rather, our data support the long-standing hypothesis that the
304 Calvin cycle is required during photoheterotrophic growth to oxidize NAD(P)H in the
305 absence of other electron-accepting processes.

306

307 **ACKNOWLEDGEMENTS**

308 We thank Gary Roberts, Di Wang, Yaoping Zhang, and Robert Kerby (University of
309 Wisconsin, Madison) for sharing strains, unpublished observations, and technical
310 guidance. We also thank Brea LaSarre for critical reading of this manuscript.

311

312 This work was supported by funds from the College of Arts and Science at Indiana
313 University (IU), including a Malcolm K. Kochert Scholarship awarded to G. C. Gordon.

314 This work was also supported in part by the Office of Science (BER), U.S. Department of
315 Energy grant DE-SC0008131. G. C. Gordon was also supported by a Hutton Honors
316 College Undergraduate Research Grant (IU), a Biology Undergraduate Research Award
317 (Cook Inc., Bloomington, IN) and a Fox Glen Research and Education Fund Award and
318 Microbiology Undergraduate Summer Research Award through the Dept. of Biology
319 (IU).

320 **REFERENCES**

- 321 1. **Muller FM.** 1933. On the metabolism of purple sulphur bacteria in organic media.
322 Arch Microbiol **4**:131–166.
- 323 2. **Calvin M.** 1962. The Path of Carbon in Photosynthesis: The carbon cycle is a tool
324 for exploring chemical biodynamics and the mechanism of quantum conversion.
325 Science. **135**:879–889.
- 326 3. **Richardson DJ, King GF, Kelly DJ, McEwan AG, Ferguson SJ, Jackson JB.**
327 1988. The role of auxiliary oxidants in maintaining redox balance during
328 phototrophic growth of *Rhodobacter capsulatus* on propionate or butyrate. Arch.
329 Microbiol. **150**:131–137.
- 330 4. **Hillmer P, Gest H.** 1977. H₂ metabolism in the photosynthetic bacterium
331 *Rhodospseudomonas capsulata*: H₂ production by growing cultures. J. Bacteriol.
332 **129**:724–31.
- 333 5. **Hallenbeck PL, Lerchen R, Hessler P, Kaplan S.** 1990. Roles of CfxA, CfxB, and
334 external electron acceptors in regulation of ribulose 1,5-bisphosphate
335 carboxylase/oxygenase expression in *Rhodobacter sphaeroides*. J. Bacteriol.
336 **172**:1736–1748.
- 337 6. **Falcone DL, Tabita FR.** 1991. Expression of endogenous and foreign ribulose 1,5-
338 bisphosphate carboxylase-oxygenase (RubisCO) genes in a RubisCO deletion
339 mutant of *Rhodobacter sphaeroides*. J. Bacteriol. **173**:2099–108.

- 340 7. **Paoli GC, Vichivanives P, Tabita FR.** 1998. Physiological Control and Regulation
341 of the *Rhodobacter capsulatus cbb* Operons. *J. Bacteriol.* **180**:4258–4269.
- 342 8. **McKinlay JB, Harwood CS.** 2010. Carbon dioxide fixation as a central redox
343 cofactor recycling mechanism in bacteria. *Proc. Natl. Acad. Sci. U. S. A.*
344 **107**:11669–11675.
- 345 9. **Laguna R, Tabita FR, Alber BE.** 2011. Acetate-dependent photoheterotrophic
346 growth and the differential requirement for the Calvin-Benson-Bassham reductive
347 pentose phosphate cycle in *Rhodobacter sphaeroides* and *Rhodospseudomonas*
348 *palustris*. *Arch. Microbiol.* **193**:151–4.
- 349 10. **McKinlay JB, Harwood CS.** 2011. Calvin cycle flux, pathway constraints, and
350 substrate oxidation state together determine the H₂ biofuel yield in
351 photoheterotrophic bacteria. *MBio.* **2**:10.1128/mBio.00323–10.
- 352 11. **Wang D, Zhang Y, Pohlmann EL, Li J, Roberts GP.** 2011. The poor growth of
353 *Rhodospirillum rubrum* mutants lacking RubisCO is due to the accumulation of ribulose-
354 1,5-bisphosphate. *J. Bacteriol.* **193**:3293–3303.
- 355 12. **Hallenbeck PL, Lerchen R, Hessler P, Kaplan S.** 1990. Phosphoribulokinase
356 activity and regulation of CO₂ fixation critical for photosynthetic growth of
357 *Rhodobacter sphaeroides*. *J. Bacteriol.* **172**:1749–61.

- 358 13. **Hädicke O, Grammel H, Klamt S.** 2011. Metabolic network modeling of redox
359 balancing and biohydrogen production in purple nonsulfur bacteria. *BMC Syst. Biol.*
360 **5**:150.
- 361 14. **Klamt S, Schuster S, Gilles ED.** 2002. Calculability analysis in underdetermined
362 metabolic networks illustrated by a model of the central metabolism in purple
363 nonsulfur bacteria. *Biotechnol. Bioeng.* **77**:734–51.
- 364 15. **Gharibi H, Atikol U, Öztürk Y, Gökçe A, Peksel B, Gürkan M, Özgür E,**
365 **Gündüz U, Eroğlu İ, Yücel M.** 2012. Hydrogen production properties of
366 *Rhodobacter capsulatus* with genetically modified redox balancing pathways. *Int. J.*
367 *Hydrogen Energy* **37**:2014–2020.
- 368 16. **Gest H.** 1999. Memoir of a 1949 railway journey with photosynthetic bacteria.
369 *Photosynth. Res.* **61**:91–96.
- 370 17. **Wang D, Zhang Y, Welch E, Li J, Roberts GP.** 2010. Elimination of Rubisco
371 alters the regulation of nitrogenase activity and increases hydrogen production in
372 *Rhodospirillum rubrum*. *Int. J. Hydrogen Energy.* **35**:7377–7385.
- 373 18. **Joshi HM, Tabita FR.** 1996. A global two component signal transduction system
374 that integrates the control of photosynthesis, carbon dioxide assimilation, and
375 nitrogen fixation. *Proc. Natl. Acad. Sci. U. S. A.* **93**:14515–20.

- 376 19. **Fitzmaurice WP, Saari LL, Lowery RG, Ludden PW, Roberts GP.** 1989. Genes
377 coding for the reversible ADP-ribosylation system of dinitrogenase reductase from
378 *Rhodospirillum rubrum*. Mol. Gen. Genet. **218**:340–347.
- 379 20. **Ormerod JG, Ormerod KS, Gest H.** 1961. Light-dependent utilization of organic
380 compounds and photoproduction of molecular hydrogen by photosynthetic bacteria;
381 relationships with nitrogen metabolism. Arch. Biochem. Biophys. **94**:449–463.
- 382 21. **Larimer FW, Chain P, Hauser L, Lamerdin J, Malfatti S, Do L, Land ML,**
383 **Pelletier DA, Beatty JT, Lang AS, Tabita FR, Gibson JL, Hanson TE, Bobst C,**
384 **Torres JL, Peres C, Harrison FH, Gibson J, Harwood CS.** 2004. Complete
385 genome sequence of the metabolically versatile photosynthetic bacterium
386 *Rhodopseudomonas palustris*. Nat. Biotechnol. **22**:55–61.
- 387 22. **Rey FE, Oda Y, Harwood CS.** 2006. Regulation of uptake hydrogenase and effects
388 of hydrogen utilization on gene expression in *Rhodopseudomonas palustris*. J.
389 Bacteriol. **188**:6143–6152.
- 390 23. **Kim M, Harwood CS.** 1991. Regulation of benzoate-CoA ligase in
391 *Rhodopseudomonas palustris*. FEMS Microbiol Lett **83**:199–203.
- 392 24. **Horton RM, Ho SN, Pullen JK, Hunt HD, Cai Z, Pease LR.** 1993. Gene splicing
393 by overlap extension. Methods Enzymol. **217**:270–279.

- 394 25. **Yanisch-Perron C, Vieira J, Messing J.** 1985. Improved M13 phage cloning
395 vectors and host strains: nucleotide sequences of the M13mp18 and pUC19 vectors.
396 *Gene* **33**:103–19.
- 397 26. **Quandt J, Hyndes MF.** 1993. Versatile suicide vectors which allow direct selection
398 for gene replacement in gram-negative bacteria. *Gene* **127**:15–21.
- 399 27. **Simon R, Prierer U, Pühler A.** 1983. A broad host range mobilization system for in
400 vivo genetic engineering: transposon mutagenesis in Gram negative bacteria. *Nat.*
401 *Biotechnol.* **1**:784–791.
- 402 28. **Huang JJ, Heiniger EK, McKinlay JB, Harwood CS.** 2010. Production of
403 hydrogen gas from light and the inorganic electron donor thiosulfate by
404 *Rhodospseudomonas palustris*. *Appl. Environ. Microbiol.* **76**:7717–7722.
- 405 29. **Karr DB, Waters JK, Emerich DW.** 1983. Analysis of poly-3-hydroxybutyrate in
406 *Rhizobium japonicum* bacteroids by ion-exclusion high-pressure liquid
407 chromatography and UV detection. *Appl. Environ. Microbiol.* **46**:1339–1344.
- 408 30. **Rey FE, Heiniger EK, Harwood CS.** 2007. Redirection of metabolism for
409 biological hydrogen production. *Appl. Environ. Microbiol.* **73**:1665–1671.
- 410 31. **Zou X, Zhu Y, Pohlmann EL, Li J, Zhang Y, Roberts GP.** 2008. Identification
411 and functional characterization of NifA variants that are independent of GlnB
412 activation in the photosynthetic bacterium *Rhodospirillum rubrum*. *Microbiology.*
413 **154**:2689–2699.

- 414 32. **Wang X, Modak H V, Tabita FR.** 1993. Photolithoautotrophic growth and control
415 of CO₂ fixation in *Rhodobacter sphaeroides* and *Rhodospirillum rubrum* in the
416 absence of ribulose bisphosphate carboxylase-oxygenase. *J. Bacteriol.* **175**:7109–14.
- 417 33. **Grammel H, Gilles E-D, Ghosh R.** 2003. Microaerophilic cooperation of reductive
418 and oxidative pathways allows maximal photosynthetic membrane biosynthesis in
419 *Rhodospirillum rubrum*. *Appl. Environ. Microbiol.* **69**:6577–6586.

Strain/Plasmid	Phenotype	Relevant genotype	Reference
<i>Escherichia coli</i>			
S17		<i>thi pro hdsR hdsM⁺ recA</i> ; RP4-2 (Tc::Mu Km::Tn7)	(27)
NEB10 β		F ⁻ λ <i>recA1</i> Δ (<i>lacZYA-argF</i>)U169 <i>hdsR17 thi-1 gyrA96 supE44 endA1 relA1</i> Φ 80 <i>lacZ</i> Δ M15	New England Biolabs
<i>Rhodopseudomonas palustris</i>			
CGA009	wild type	<i>hupV⁻</i>	(21, 22)
CGA4007	Δ PRK	Δ <i>cbbP</i> ::Km <i>hupV⁻</i>	This study.
CGA676	NifA*	<i>nifA</i> * <i>hupV⁻</i>	(8)
CGA678	NifA* Δ Rubisco II	<i>nifA</i> * Δ <i>cbbM</i> <i>hupV⁻</i>	(8)
CGA4010	NifA* Δ PRK	<i>nifA</i> * Δ <i>cbbP</i> ::Km ^R <i>hupV⁻</i>	This study.
CGA4009	NifA* Δ Rubisco	<i>nifA</i> * Δ <i>cbbLS</i> Δ <i>cbbM</i> <i>hupV⁻</i>	This study.
CGA4011	NifA* Δ Rubisco Δ PRK	<i>nifA</i> * Δ <i>cbbLS</i> Δ <i>cbbM</i> Δ <i>cbbP</i> ::Km ^R <i>hupV⁻</i>	This study.
<i>Rhodospirillum rubrum</i>			
UR2	wild type		(19)
UR2565	Δ PRK	Δ <i>cbbP</i> ::Km ^R	(11)
UR5251	Δ Rubisco	Δ <i>cbbM</i> ::Gm ^R	(17)
UR2557	Δ Rubisco Δ PRK	Δ <i>cbbM</i> ::Gm ^R Δ <i>cbbP</i> ::Km ^R	(11)

420

421 **Table 1. Strains used in this study.** *Rp. palustris* encodes both Rubisco type I (*cbbLS*)

422 and type II (*cbbM*). CGA678 (NifA* Δ Rubisco II) still has Rubisco activity due to

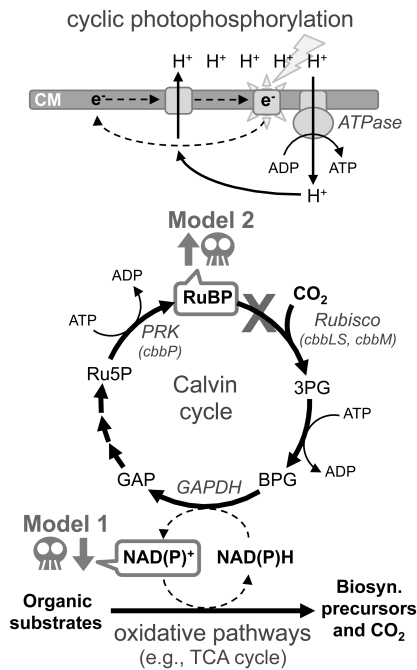
423 *cbbLS*. Any *R. palustris* strain designated, Δ Rubisco (e.g., CGA4009 and CGA4011)

424 lacks both *cbbM* and *cbbLS* and does not have Rubisco activity.

425 **Table 2. Plasmids and primers used in this study.**

Plasmid/Primer	Features/Sequence (5' – 3')	Ref./ description
pBBPgdh	Gm ^R ; mobilizable broad-host-range cloning vector with a constitutive <i>Rp. palustris</i> promoter	(8)
pJQ200SK	Gm ^R , <i>sacB</i> ; mobilizable <i>Rp. palustris</i> suicide vector	(26)
pUC19	Ap ^R ; High-copy-number cloning vector	(25)
pGEM	High-copy-number cloning vector for direct insertion of PCR products	Promega
pPS858_Km2	Ap ^R ; Km ^R ; FRT	(8)
pGEM <i>cbbP</i>	Ap ^R ; <i>cbbP</i> and ribosomal binding site cloned into pGEM	
pBBP <i>cbbP</i>	Gm ^R ; derived from pBBPgdh; complementation vector for $\Delta cbbP::Km^R$	This study.
pUC $\Delta cbbLS$	Ap ^R ; in-frame $\Delta cbbLS$ cloned into XbaI/BamHI sites of pUC19	This study.
pGEM $\Delta cbbP$	Ap ^R ; in-frame $\Delta cbbP$ cloned into pGEM	This study.
pGEM $\Delta cbbP::Km^R$	Ap ^R , Km ^R ; in-frame $\Delta cbbP::Km^R$ in pGEM	This study.
pJQ $\Delta cbbLS$	Gm ^R ; in-frame $\Delta cbbLS$ cloned into pJQ200SK	This study.
pJQ $\Delta cbbP::Km^R$	Gm ^R ; in-frame $\Delta cbbP::Km^R$ cloned into pJQ200SK	This study.
JBM47	aaagcaagccgctctagacatcaacg	$\Delta cbbLS$ upstream primer (XbaI)

JBM48	gttcatgtcgtcctccttgaagcc	$\Delta cbbLS$ in-frame deletion reverse
JBM49	caaggaggacgacatgaacggctgatcgtggacgcgacagc	$\Delta cbbLS$ in-frame deletion forward
JBM50	gtcgcgcgaattgtggatccaacgt	$\Delta cbbLS$ downstream primer (<u>BamHI</u>)
JBM128	gctgCaggatgtgccgtacgc	$\Delta cbbP$ upstream primer (<u>PstI</u>)
JBM129	gtttgcggtcgcaggtaccgatggagatgatcggatgcttac	$\Delta cbbP$ in-frame deletion reverse (<u>KpnI</u>)
JBM130	ccgatcatctccatcggtagctgatcgaccgcaaacgaagcatg	$\Delta cbbP$ in-frame deletion forward (<u>KpnI</u>)
JBM131	cttctagacctcgtcggegcc	$\Delta cbbP$ downstream primer (<u>XbaI</u>)
GG010	ggatccacgtcgtctctccggt	<i>cbbP</i> complementation forward (<u>BamHI</u>)
GG011	tctagacgtgcgggaacgttcaaa	<i>cbbP</i> complementation reverse (<u>XbaI</u>)
JBM114	aggtaccaattccgcgaacccaga	Km ^R from pPS858_Km2 forward (<u>KpnI</u>)
JBM115	tggtagcaattccgctagcttcacgct	Km ^R from pPS858_Km2 reverse (<u>KpnI</u>)



427

428 **Figure 1. Two models to explain why disrupting Rubisco activity prevents**

429 **photoheterotrophic growth in PNSB.** In both models, ATP generation is decoupled

430 from central metabolism as electrons are repeatedly energized and cycled through a H⁺-

431 pumping electron transfer chain (cyclic photophosphorylation; top). Oxidative pathways

432 convert organic substrates into biosynthetic precursors and CO₂ and reduce electron

433 carriers (bottom). The Calvin cycle generates biosynthetic precursors, fixes CO₂, and

434 oxidizes electron carriers (middle). In model 1, disrupting Rubisco activity (gray X)

435 prevents Calvin cycle flux leading to a depletion of oxidized electron carriers that halts

436 all metabolic activity. In model 2, disrupting Rubisco activity leads to a lethal

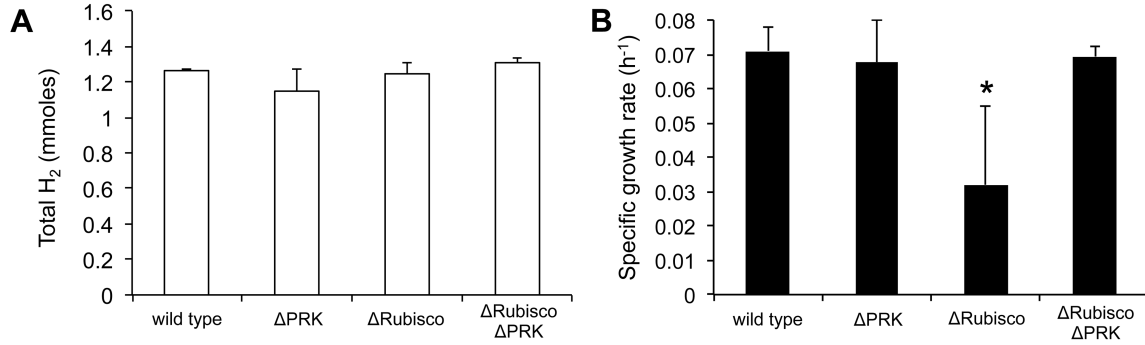
437 accumulation of toxic RuBP, produced by PRK. BPG, 1,3-bisphosphoglycerate; CM,

438 cytoplasmic membrane; GAP, glyceraldehyde-3-phosphate; GAPDH, GAP

439 dehydrogenase; PRK, phosphoribulokinase; R5P, ribulose-5-phosphate; RuBP, ribulose-

440 1,5-bisphosphate; Rubisco, ribulose-1,5-bisphosphate carboxylase; TCA, tricarboxylic

441 acid.



442

443 **Figure 2. Preventing RuBP accumulation using a Δ PRK mutation improved the**
 444 **growth rate of a *Rs. rubrum* Δ Rubisco mutant under conditions permitting H₂**

445 **production. *Rs. rubrum* strains were grown phototrophically in minimal medium with**

446 **malate and glutamate. A. H₂ levels measured at the onset of stationary phase (i.e., when**

447 **the highest OD₆₆₀ value was observed). Values are averages from three biological**

448 **replicates with error bars representing standard deviations. B. Average specific growth**

449 **rates from 3-5 biological replicates with error bars representing standard deviations. The**

450 *** indicates that a value was significantly different from that of the wild-type (p -value <**

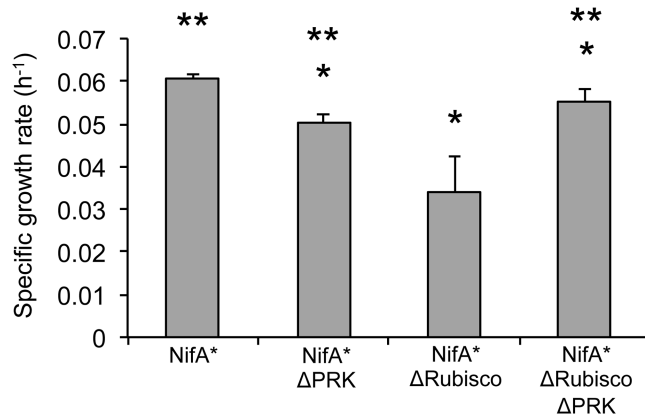
451 **0.05; two-tailed t -test, equal variance). Wild type, UR2; Δ PRK, UR2565 (Δ *cbbP*::Km^R);**

452 **Δ Rubisco, UR5251 (Δ *cbbM*::Gm^R); Δ Rubisco Δ PRK, UR2557 (Δ *cbbM*::Gm^R,**

453 **Δ *cbbP*::Km^R).**

454

455

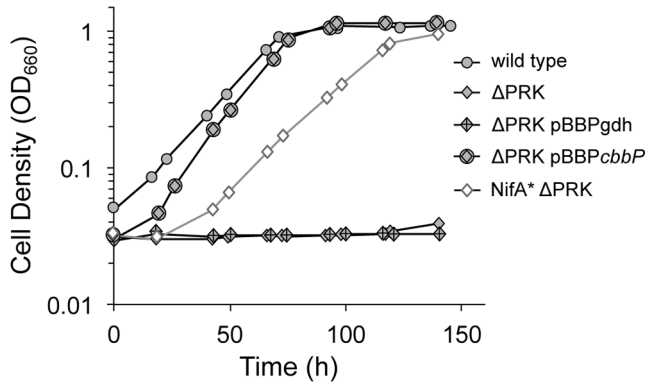


456

457 **Figure 3. Preventing RuBP accumulation using ΔPRK mutations improved the**
458 **growth rate of a H₂-producing *Rp. palustris* NifA* ΔRubisco mutant.** Average
459 specific growth rates from three biological replicates with error bars representing
460 standard deviations. *Rp. palustris* strains were grown phototrophically in minimal
461 medium with succinate and NH₄⁺. All strains produced H₂ during growth due to a *nifA**
462 mutation. The * indicates that a value was significantly different from that of the NifA*
463 parent (*p*-value < 0.05; two-tailed *t*-test, equal variance). The ** indicates that a value was
464 significantly different from that of the NifA* ΔRubisco strain (*p*-value < 0.05; two-tailed
465 *t*-test, equal variance). NifA*, CGA676 (*nifA**); NifA* ΔPRK (*nifA**, Δ*cbbP*::Km^R),
466 CGA4010; NifA* ΔRubisco, CGA4009 (*nifA**, Δ*cbbLS*, Δ*cbbM*); NifA* ΔRubisco
467 ΔPRK, CGA4011 (*nifA**, Δ*cbbLS*, Δ*cbbM*, Δ*cbbP*::Km^R).

468

469



470

471 **Figure 4. A Δ PRK mutant of *Rp. palustris* that cannot produce RuBP was incapable**

472 **of photoheterotrophic growth unless H_2 production was permitted. *Rp. palustris***

473 strains were grown in a minimal medium with malate and NH_4^+ . Only the NifA* strain

474 can produce H_2 under these growth conditions. Representative values from single

475 biological replicates are shown. Similar trends were observed for at least three biological

476 replicates. Wild type, CGA009; Δ PRK, CGA4007 ($\Delta cbbP::Km^R$); Δ PRK pBBPgdh ,

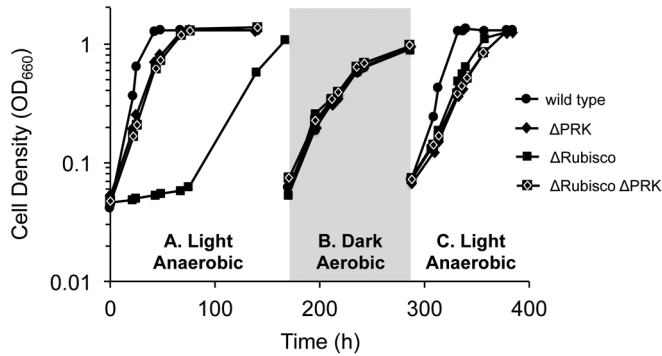
477 CGA4007 ($\Delta cbbP::Km^R$) with empty vector (Table 2) Δ PRK pBBPcbbP, CGA4007

478 ($\Delta cbbP::Km^R$) with complementation vector (Table 2); NifA* Δ PRK, CGA4010 (*nifA**,

479 $\Delta cbbP::Km^R$).

480

481



482

483 **Figure 5. *Rs. rubrum* Calvin cycle mutants grew photoheterotrophically on malate**

484 **with NH₄⁺ without producing H₂.** *Rs. rubrum* strains were grown aerobically in rich

485 SMN medium and then transferred to anaerobic phototrophic minimal medium with

486 malate and NH₄⁺ (A. Light Anaerobic). Cultures were then transferred to aerobic, rich

487 SMN medium and allowed to grow (B. Dark Aerobic) before being transferred to the

488 same conditions as in A (C. Light Anaerobic). Representative data from single biological

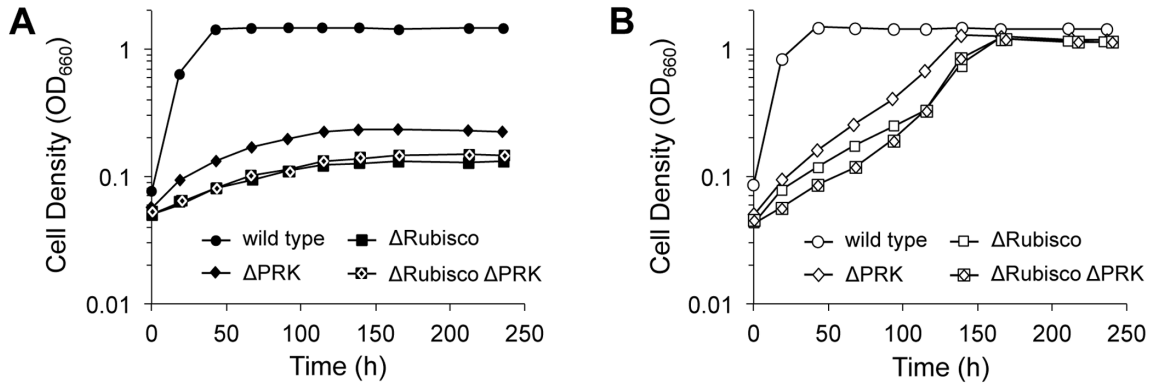
489 replicates are shown. Similar trends were observed for at least three biological replicates

490 for each trend except that the initial ΔRubisco strain lag phase ended at different times.

491 No culture produced more than 2.5 μmoles of H₂.

492

493



494

495 **Figure 6. *Rs. rubrum* Calvin cycle mutants could not grow photoheterotrophically**
496 **with succinate and NH₄⁺ (A) unless DMSO was provided as an electron acceptor (B).**

497 Cultures with succinate and NH₄⁺ were inoculated from cultures grown phototrophically
498 with malate and NH₄⁺, but without DMSO (Fig. 5). Representative data from single
499 biological replicates are shown. Similar trends were observed for at least three biological
500 replicates. **A.** no DMSO; **B.** DMSO added.